Inorganic Chemistry

Article

pubs.acs.org/IC

$[Li(XeF_2)_n](AF_6)$ (A = P, As, Ru, Ir), the First Xenon(II) Compounds of Lithium. Synthesis, Raman Spectrum, and Crystal Structure of $[Li(XeF_2)_3](AsF_6)$

Gašper Tavčar* and Boris Žemva

Department of Inorganic Chemistry and Technology, Jožef Stefan Institute, Jamova 39, SI-1000 Ljubljana, Slovenia

Supporting Information

ABSTRACT: The reactions between compounds of the type MAF_6 (M = alkali metal; A = P, As, V, Ru, Ir, Sb, Nb, Ta) and xenon difluoride were studied in anhydrous hydrogen fluoride solvent. The coordination products $[M(XeF_2)_n]AsF_6$ were only observed in the case of $LiAF_6$ (A = P, As, Ru, Ir), and the crystal structure of $[Li(XeF_2)_3]AsF_6$ was determined (monoclinic space group $P2_1$ with a = 6.901(9) Å, b = 13.19(2) Å, c = 6.91(1) Å, β = 91.84(2)°, and Z = 2). The coordination sphere of lithium is comprised of six F atoms. The compound series was also characterized by Raman spectroscopy.

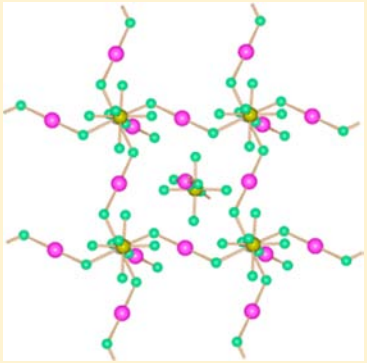

INTRODUCTION

Complexes of the alkali-metal fluorides with xenon fluorides are known only for Xe^{IV} and Xe^{VI}, as exemplified by the salts $MXeF_5$ (M = Na, K, Rb, Cs),[1] $MXeF_7$ (M = Rb, Cs),[2−5] and M_2XeF_8 (M = Na, K, Rb, Cs).[2−4] Until now, compounds between alkali-metal fluorides and XeF_2 were unknown.

Xenon difluoride, as a ligand bonded directly to a metal ion, was first observed in $[Ag(XeF_2)_2]AsF_6$,[6] and a variety of further metal salts with XeF_2 coordinated to metal ions have been discussed in a recent review.[7] However, the only complexes of XeF_2 with M^+ ions are those of Ag^I.[6,8]

In this paper, we report the first coordination compound in which XeF_2 functions as a ligand toward the Li^+ ion in the presence of different AF_6 (A = P, As, Ru, Ir) anions.

EXPERIMENTAL SECTION

General Experimental Procedures. A nickel vacuum line coupled to a mechanical pump and an oil diffusion pump was used to carry out the reactions. Fluorine and volatile fluorides were removed with a soda lime scrubber and liquid-nitrogen cold traps. Volatile AF_5 compounds and anhydrous hydrogen fluoride (aHF) were handled on a part of the vacuum line made from Teflon, polyfluoroethylene, and hexafluoropropylene−tetrafluoroethylene copolymer (FEP) in order to diminish corrosion. Pressures were measured by means of a Monel Helicoid pressure gauge (0−3000 Torr ± 0.25%) connected to the vacuum manifold with a Teflon valve. Moisture-sensitive materials were handled in the dry argon atmosphere of a glovebox (water content of ≤0.1 ppm; M. Braun, Garching, Germany). Reaction vessels, made of PFA and equipped with Teflon valves and Teflon-coated stirring bars, were used for syntheses. Crystals were grown in a crystallization vessel, made from a T-shaped FEP reaction vessel constructed from a 16-mm-i.d. length of the FEP tube and a length of 4-mm-i.d. FEP tubing connected to a Teflon valve. Saturated solutions in aHF were decanted from one arm of the crystallization vessel to the other. A temperature gradient was maintained between both arms in order to induce crystal growth. Alternatively, smaller vessels for crystal growth were fabricated from FEP tubing using 10 cm and 4-mm-i.d. lengths.

Reagents. Lithium fluoride was obtained from British Drug Houses Ltd. (99% purity). Xenon difluoride was prepared by the photochemical reaction of xenon with difluoride at room temperature.[9] aHF (Fluka, purum) was treated with K_2NiF_6 (Ozark-Mahoning, 99%) for several days prior to use. Arsenic pentafluoride and PF_5 were synthesized by pressure fluorination of As_2O_3 (Alfa Aesar, 99%) or P_2O_5 (Sigma-Aldrich, ≥98.0%) with difluoride in a nickel reactor at 300 °C as previously described.[10]

Caution! *Reactions with aHF, AF_5 (A = P, V, As, Ru, Ir, Sb, Nb, Ta), and XeF_2 must be carried out in a well-ventilated hood, and protective clothing must be worn at all times. The experimentalist must become familiar with these reagents and the hazards associated with them. Fresh tubes of calcium gluconate gel should always be on hand for the immediate treatment of skin exposed to these reagents. For a full protocol for the treatment of HF exposure, see ref 11.*

Syntheses of $LiAF_6$ (A = P, V, As). $LiAF_6$ was synthesized from LiF (0.1202 g, 4.64 mmol) and a excess of gaseous AF_5 (PF_5; 0.7610 g, 6.04 mmol) in aHF solvent.[12] After the reaction was completed, the excess MF_5 and solvent were pumped off on the vacuum line. The product was verified by mass balance, powder X-ray diffraction, and Raman spectroscopy (Figure 1).

Syntheses of $LiAF_6$ (A = Sb, Ru, Ir, Nb, Ta). $LiAF_6$ was synthesized from LiF (0.0623 g, 2.405 mmol) and stoichiometric amounts of either elemental A or AF_3 (Ru: 0.2393 g, 2.369 mmol), which were subsequently fluorinated with difluoride in aHF solvent. The reactions were monitored by mass balance, and the product was

Received: October 22, 2012
Published: March 29, 2013

   dx.doi.org/10.1021/ic302323j | Inorg. Chem. 2013, 52, 4319−4323

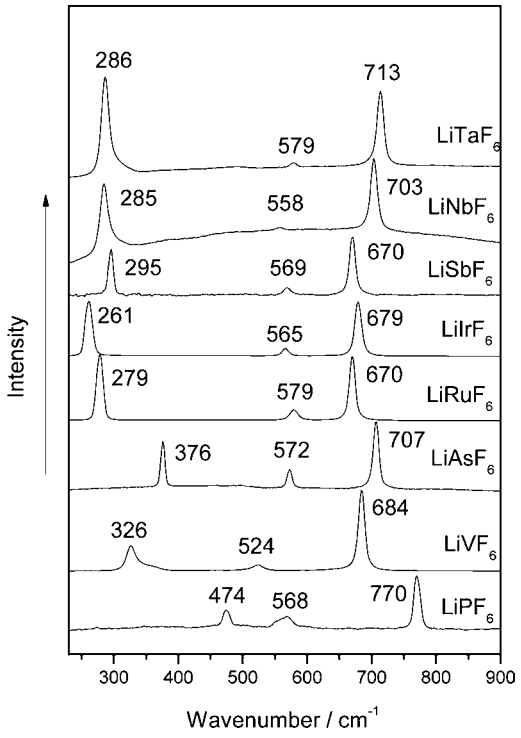

Figure 1. Comparison of the Raman spectra of $LiAF_6$ (A = P, As, V, Ru, Ir, Sb, Nb, Ta).

characterized by powder X-ray diffraction and Raman spectroscopy (Figure 1).

Syntheses of $[Li(XeF_2)_n]AF_6$ (A = P, As, Ru, Ir). The syntheses were carried out using $LiAF_6$ salts (see above) and excess amounts of XeF_2 in aHF solvent. The $[Li(XeF_2)_n]AF_6$ (A = As, Ru, Ir) complexes were isolated at room temperature, where they slowly lost XeF_2, yielding $LiAF_6$. The compound $[Li(XeF_2)_n]PF_6$ was isolated at −30 °C, but at ca. −14 °C, it rapidly decomposed to $LiPF_6$ and XeF_2, as can be seen from its Raman spectrum at that temperature.

Growth of Single Crystals of $[Li(XeF_2)_3]AsF_6$. Stoichiometric amounts of $LiAsF_6$ and XeF_2 were placed in a narrow FEP tube and dissolved in aHF. The vessel was cooled to −50 °C, and aHF solvent was slowly pumped off on the vacuum line at a rate of approximately 1 mL/day. The resulting powder contained small crystals and was immersed in perfluorinated oil (ABCR, FO5960) in a drybox. A suitable crystal was selected under the microscope and transferred into the cold nitrogen stream of the X-ray diffractometer.

Crystal Structure Determination. A single-crystal X-ray data set was collected for $[Li(XeF_2)_3]AsF_6$ using a Mercury CCD area detector coupled to a Rigaku AFC7 diffractometer using graphite-monochromated Mo Kα radiation (λ = 0.71069 Å). The data were corrected for Lorentz and polarization effects. A multiscan absorption correction was applied to the data sets. All calculations during the data processing were performed using the *CrystalClear* software suite.[13] Structures were solved using direct methods[14] and expanded Fourier techniques. Full-matrix least-squares refinement of F^2 against all reflections was performed using the *SHELX 97* program.[15]

Crystal structure data for the compound was collected at −73 °C. Details of the data collection and structure refinement are given in Table 1 and the Supporting Information.

Raman Spectroscopy. Raman spectra of powdered samples in sealed quartz capillaries or in an FEP reaction vessel ($[Li(XeF_2)_n]PF_6$) were recorded on a Renishaw Raman Imaging Microscope System 1000 using the 632.8 nm line of a He−Ne laser for excitation. The geometry for all of the Raman experiments was 180° backscattering with a laser power of 25 mW.

Powder X-ray Diffraction Patterns. Diffraction data were recorded for powdered samples in sealed quartz capillaries using a 143-mm Debye-Scherer camera with X-ray film and Cu Kα radiation. The intensities were visually estimated.

Table 1. Crystal Data and Structure Refinement of $[Li(XeF_2)_3]AsF_6$[a]

a (Å)	6.901(9)
b (Å)	13.19(2)
c (Å)	6.91(1)
β (deg)	91.84(2)
V (Å^3)	628(2)
Z	2
fw	703.76
space group	$P2_1$
T (°C)	−73(1)
λ (Å)	0.71069
ρ_{calcd} (g/cm^3)	3.720
μ (mm^{-1})	10.778
R1	0.0531
wR2	0.1324

[a] $R1 = \sum||F_o| - |F_c||/\sum|F_o|$; $wR2 = [\sum(w(F_o^2 - F_c^2)^2)/\sum w(F_o^2)^2]^{1/2}$.

RESULTS AND DISCUSSION

Synthesis. Only the coordination compounds $[Li(XeF_2)_n](AF_6)$ (A = As, Ru, Ir) were isolated from mixtures of $MAsF_6$ (M = Li, Na, K, Rb, Cs) and XeF_2 in aHF solvent. They slowly lost XeF_2 at room temperature, yielding $LiAF_6$. However, $[Li(XeF_2)_n]PF_6$ can be isolated at −30 °C, but at ca. −14 °C, it rapidly decomposes, yielding $LiPF_6$ and XeF_2. Among the other alkali metals, only sodium indicated formation of a XeF_2 coordination compound.

Sodium hexafluoroarsenate does not completely dissolve in aHF but dissolves after the addition of XeF_2, indicating that a coordination compound is probably formed. It was not possible to establish the existence of this compound by Raman spectroscopy after the solvent was removed at −50 °C. The only vibrational bands seen correspond to free XeF_2 and $NaAsF_6$.

In general, it is noted that the smaller the formula unit volume of the salt, the greater the lattice energy. Therefore, small cations should be more favorable than larger. Moreover, a small cation has a greater polarizing power than a larger one. Thus, Li^+ polarizes the nonbridging XeF_2 more than Na^+, providing a further explanation for the existence of the lithium compound. Another factor contributing to the exclusion of the other alkali metals from XeF_2 complex formation is the absolute electronegativities of these cations, which are significantly higher in the case of Li^+ (40.52 eV) than those of the other alkali-metal ions (Na^+ = 26.21 eV; K^+ = 17.99 eV; Cs^+ = 14.5 eV), suggesting that electron density donation from XeF_2 to Li^+ will be higher than that in the case of the heavier alkali-metal cations.[16]

The coordination number of Li^+ will tend to be lower than those for the heavier cations. The $LiAF_6$ salts have NaCl-type lattices in which Li^+ is octahedrally coordinated by F^- ligands, whereas for the K^+, Rb^+, and Cs^+ salts, the lattice type is commonly CsCl, albeit rhombohedral, with eight or more F atoms in the cation coordination sphere.

Slow crystallization (temperature gradient 10 °C) from saturated solutions of $[Li(XeF_2)_3]AsF_6$ in aHF always resulted in single crystals of $LiAsF_6$. The formation of $[Li(XeF_2)_3]AsF_6$ is therefore most likely kinetically favorable, while the formation of $LiAsF_6$ is thermodynamically preferred. Therefore,

dx.doi.org/10.1021/ic302323j | Inorg. Chem. 2013, 52, 4319−4323

only a few suitable crystals of $[Li(XeF_2)_3]AsF_6$ were obtained during rapid crystallization from saturated solutions.

The influence of the AF_6^- anion on the structural diversity of coordination compounds of the type $[Li(XeF_2)_n](AF_6)$ is also important but to a lesser extent than that of the cation. The reactions of $LiAF_6$ (A = P, V, Ru, Ir, Sb, Nb, Ta) salts and XeF_2 in aHF solvent were also studied. Coordination compounds of the type $[Li(XeF_2)_n](AF_6)$ were only obtained in the case where A is P, Ru, and Ir. On the basis of their Raman spectra, they are most likely isostructural with $[Li(XeF_2)_3]AsF_6$. Raman spectroscopy shows that all compounds in this series are unstable and decompose with time at room temperature to $LiAF_6$ and XeF_2. The most stable compound is $[Li(XeF_2)_3](AsF_6)$, which is still possible to detect by Raman spectroscopy after several weeks at room temperature. To account for this behavior, the Lewis basicity of AF_6^-, the size of the anion, the charge on the F^- ligands of AF_6^-, and the solubilities of the parent $LiAF_6$ salts should be considered. Because the lattice energy (U) is roughly proportional to the inverse of the cube root of the formula unit volume, the U term is not likely to be much diminished for the larger AF_6^- relative to the smaller anion. The greater difference could derive from the differing F^- ligand charges. For example, in SbF_6^-, the charge on the F atom must be greater than that in PF_6^-. So, when SbF_6^- approaches a cation, it competes more effectively in displacing XeF_2 than PF_6^- does. On the other hand, a larger anion size could increase repulsion forces between F atoms in the crystal structure.

The structure of $[Li(XeF_2)_3](AsF_6)$ consists of $Li_4(XeF_2)_4$ squares connected to form layers, with the XeF_2 molecule and AsF_6 unit from two neighboring layers pushed toward this square. If the volume of the anion inserted into the square would increase, so would the repulsive forces between the F atoms. Changing the anion to SbF_6^-, for instance, should increase the A–F distance from approximately 1.74(4) Å in $LiAsF_6$[17] to 1.877(6) Å in $LiSbF_6$,[18] an increase of 0.13 Å. This could decrease the shortest F(As) to F(Xe) distance to approximately 2.57 Å, which may be enough to shift the equilibrium toward the formation of $LiSbF_6$.

There are other factors, such as the relative solubilities of the parent $LiAF_6$ salts in aHF, that also affect the success or failure of the synthetic approach that has been used. The solubility data for $LiAF_6$ salts are incomplete. Heavier $LiAF_6$ (A = Sb, Bi, Ta, Nb) salts often have lower solubilities, which could also account for the nonexistence of these coordination compounds. Similar behavior was observed in the case of silver(I) coordination compounds with XeF_2, where it was possible to prepare $[Ag(XeF_2)_2]AF_6$ (A = P, As), but no indication of XeF_2 coordination was observed in the cases of A = Sb, Nb, and Ta.[8] Most probably, the reasons for such behavior in the Li^+ series of XeF_2 complexes are the same.

One must take care not to overgeneralize based on the apparent nonexistence of these compounds. It may simply be that one has not found the correct conditions for kinetic stabilization of what are, in most cases, thermodynamically unstable salts.

Crystal Structure of $[Li(XeF_2)_3]AsF_6$. The coordination sphere around the Li atom consists of six F atoms (one AsF_6^- unit and five XeF_2 molecules; Figure 2). There is only one nonbridging XeF_2 molecule, coordinated to the Li atom through an F ligand, with a Li–F(Xe) distance of 2.07(3) Å. In the four bridging XeF_2 molecules, the bridging Li–F(Xe) distances range from 1.97(2) to 2.03(3) Å.

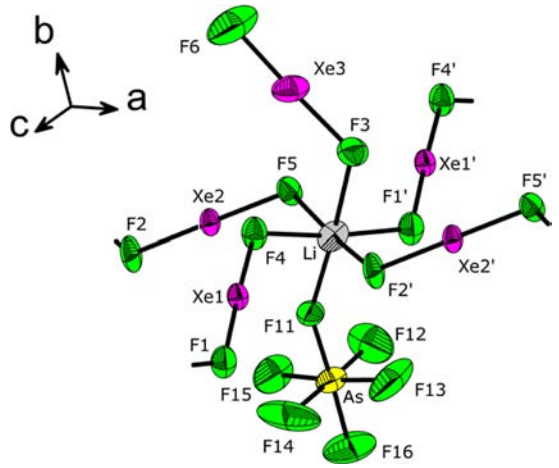

Figure 2. Coordination sphere of Li in $[Li(XeF_2)_3]AsF_6$. Thermal ellipsoids are drawn at the 50% probability level.

Bridging XeF_2 molecules link the Li atoms, forming infinite layers perpendicular to the b axis. The layers are shifted diagonally along the ac plane, placing AsF_6^- anions and nonbridging XeF_2 molecules in the middle of the $Li_4(XeF_2)_4$ squares of the neighboring layers (Figure 3). The layers are

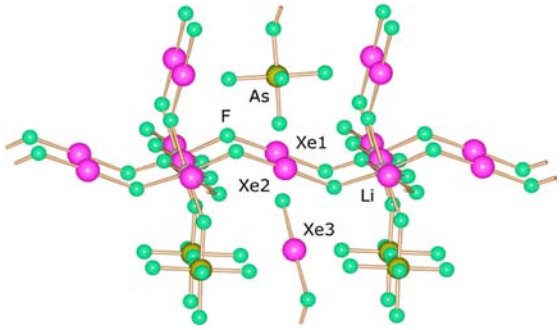

Figure 3. Packing of the layers in the structure of $[Li(XeF_2)_3]AsF_6$.

linked by electrostatic interactions between the positively charged Xe atoms of the XeF_2 molecules and negatively charged F atoms of the XeF_2 molecules and AsF_6^- anions. There are seven Xe1···F contacts in the range 3.18(3)–3.60(1) Å, five Xe2···F contacts in the range 3.28(1)–3.40(2) Å, and four Xe3···F contacts in the range 3.32(1)–3.61(3) Å.

All known isostructural $LiAF_6$ (A = P, As, Ru, Ir, Sb, Nb, Ta)[18,19] compounds for which crystal structures have been determined crystallize in the space group $R\bar{3}$. The Li cation is coordinated to six F atoms of the AF_6 units. The previously reported Li–F(AF_6) distances obtained from single-crystal structures are 2.047(1) Å (PF_6^-)[17] and 2.035 Å (IrF_6^-),[20] while the corresponding distance determined by Rietveld refinement for Li(AsF_6) powder is 2.04(5) Å, which is longer than the Li–F(AsF_6) distance in $[Li(XeF_2)_3](AsF_6)$, which is 1.92(3) Å. The large octahedral AsF_6^- ion pushes the equatorial bridging XeF_2 molecules toward the nonbridging XeF_2, as indicated by the (XeF_2)F–Li–F(AsF_6) angles, which are generally greater than 90° [89(1), 93(1), 94(1), and 98(1)°].

The (Li)F–Xe bridging distances are in the range 1.976(8)–2.005(8) Å, which is in a range similar to that reported for (Ag)F–Xe [1.979(3) Å] and similar to all bridging distances in coordination compounds of M^{2+} containing hexafluoroanions and bridging XeF_2 ligands. The real difference can be seen in

dx.doi.org/10.1021/ic302323j | Inorg. Chem. 2013, 52, 4319–4323

the nonbridging XeF_2 molecule, where the (Li)F−XeF distance is not elongated [2.00(1) Å], whereas the nonbridging FXe−F distance is shortened to 1.95(1) Å, which is the usual distance for nonbridging XeF_2 molecules coordinated to metal centers. The (M)F−XeF distances for M = Cd [2.043(6)−2.079(6) Å],[21,22] Mg [2.051(4)−2.079(9) Å],[23] Zn [2.078(5) Å],[24] and Cu [2.083(3)−2.102(5) Å][24,25] are actually longer than 2.00(1) Å, as seen in the lithium coordination compound. The $[Ca(XeF_2)_4](AsF_6)_2$ compound is the only compound with XeF_2 coordinated to the metal center in which similar short (M)F−XeF [2.000(9) Å] distances are found.[26]

Raman Spectroscopy. The Raman spectrum of $[Li(XeF_2)_3](AsF_6)$ is shown in Figure 4. The high polarizability

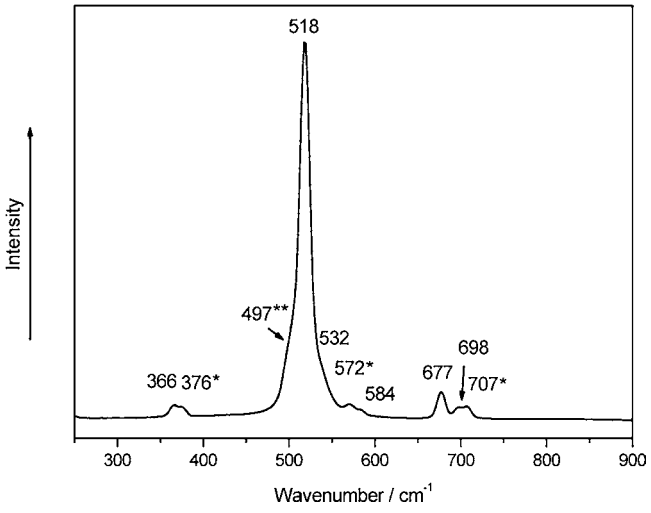

Figure 4. Raman spectrum of $[Li(XeF_2)_3]AsF_6$: *, $LiAsF_6$; **, free XeF_2.

of xenon usually results in intense Raman bands for the symmetric Xe−F stretching modes. Modes involving As−F and Li−F vibrations are usually far less intense and broader. Because of thermal decomposition of the compound to $LiAsF_6$ and XeF_2, both decomposition products are also present in the Raman spectrum of $[Li(XeF_2)_3](AsF_6)$ (Figure 4). Four XeF_2 (Xe1 and Xe2) are bridging, while one XeF_2 (Xe3) is nonbridging (Figure 2). The totally symmetric (Σ_g^+) stretching mode for XeF_2 occurs at 497 cm^{-1}.[27] When the nonbridging XeF_2 molecule is distorted by interaction of one F atom with the metal ion, the band at 497 cm^{-1} is replaced by two bands. The one at higher frequency is assigned to the stretch of the shorter Xe−F bond [ν(Xe−F)], and the band at lower frequency corresponds to the stretch of the longer Xe−F bond [ν(Xe···F)]. In XeF^+ salts, one F ligand is effectively removed from the XeF_2 molecule and the $(Xe-F)^+$ stretching frequency is normally higher than 600 cm^{-1}.[28]

In the case of the present compound, the small shoulder at 532 cm^{-1} can be assigned to the nonbridging Xe(3)F_2 molecule [ν(Xe−F)], whereas the Xe−F stretch [ν(Xe···F)] is expected at approximately 476 cm^{-1} but is probably hidden under the broader base of the most intense peak at 518 cm^{-1}. The latter peak is assigned to the Xe−F stretching modes of the four bridging XeF_2 molecules. The symmetric stretching mode of the bridging XeF_2 molecule might have been expected to be close to the value of free XeF_2. However, because the bridging XeF_2 molecules in the Li···F−Xe−F···Li moieties are anchored between two Li^+ ions, a higher energy is required for the symmetric stretching mode, resulting in an increase in the stretching frequency. The decomposition products "free" XeF_2 [497 (sh) cm^{-1}] and $LiAsF_6$ [707, 572 (sh) and 376 cm^{-1}] could also be observed in the Raman spectrum.

The AsF_6^- modes of $LiAsF_6$ are ν_1 (707 cm^{-1}), ν_2 (572 cm^{-1}), and ν_5 (376 cm^{-1}). The corresponding modes for the ideal octahedral O_h symmetry of AsF_6^- occur at ν_1, 689 cm^{-1}; ν_2, 573 cm^{-1}; and ν_5, 375 cm^{-1}.[29] Modes at 698, 677, 584, and 366 cm^{-1} are assigned to the AsF_6^- unit in $[Li(XeF_2)_3]AsF_6$. The O_h symmetry of AsF_6^- in the coordination compound is reduced to lower symmetry, resulting in more Raman-active modes.[30−32]

The Raman spectra of $[Li(XeF_2)_n]PF_6$, $[Li(XeF_2)_n]RuF_6$, and $[Li(XeF_2)_n]IrF_6$ show Xe−F stretching bands that are similar to those of $[Li(XeF_2)_3]AsF_6$ (Figure 5 and Tables 2 and

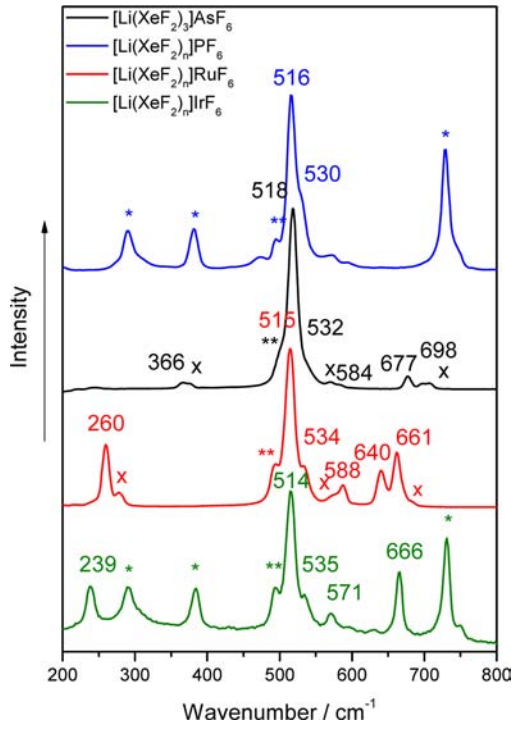

Figure 5. Comparison of the Raman spectra of $[Li(XeF_2)_3]AsF_6$, $[Li(XeF_2)_n]PF_6$, $[Li(XeF_2)_n]RuF_6$, and $[Li(XeF_2)_n]IrF_6$: *, FEP reaction vessel; **, free XeF_2; ×, $LiAF_6$.

3). This implies that all compounds in the series are most probably isostructural. The bands assigned to nonbridging XeF_2 are in range 535−530 cm^{-1}, while the bands for bridging XeF_2

Table 2. Key Raman Bands for $[Li(XeF_2)_n](AF_6)$ (A = As, P, Ru, Ir)[a]

AF_6	AsF_6	PF_6	RuF_6	IrF_6
terminal (Xe−F)	532 (23)	530 (42)	534 (26)	535 (24)
bridging (Xe−F)	518 (100)	516 (100)	515 (100)	514 (100)
AF_6^-	698 (3)		661 (35)	666 (41)
	677 (7)		640 (23)	
	584 (3)		588 (15)	571 (11)
	366 (4)		260 (39)	239 (31)

[a]Vibrational frequencies are in cm^{-1}, and relative intensities are given in parentheses.

dx.doi.org/10.1021/ic302323j | Inorg. Chem. 2013, 52, 4319−4323

Table 3. Comparison of the Raman Bands of $LiAF_6$ (A = P, V, As, Sb, Ru, Ir, Nb, Ta) in the Solid State[a]

	$LiPF_6$	$LiVF_6$	$LiAsF_6$	$LiRuF_6$	$LiIrF_6$	$LiSbF_6$	$LiNbF_6$	$LiTaF_6$
ν_1	770 (100)	684 (100)	707 (100)	670 (95)	679 (98)	670 (100)	703 (100)	713 (76)
ν_2	568 (21)	524 (10)	572 (27)	579 (16)	565 (17)	569 (16)	558 (8)	579 (7)
ν_5	474 (32)	326 (34)	376 (68)	279 (100)	261 (100)	295 (79)	285 (90)	286 (100)

[a]Vibrational frequencies are in cm^{-1}, and relative intensities are given in parentheses.

are in range 518−514 cm^{-1}. The bands for PF_6^- were not observed because of their low intensities.

■ ASSOCIATED CONTENT

Supporting Information

X-ray crystallographic file in CIF format. This material is available free of charge via the Internet at http://pubs.acs.org.

■ AUTHOR INFORMATION

Corresponding Author

*E-mail: gasper.tavcar@ijs.si. Phone: +386 1 4773225.

Notes

The authors declare no competing financial interest.

■ ACKNOWLEDGMENTS

The authors gratefully acknowledge the Slovenian Research Agency (ARRS) for financial support of the Research Program P1-0045 (Inorganic Chemistry and Technology).

■ REFERENCES

(1) Christe, K. O.; Curtis, E. C.; Dixon, D. A.; Mercier, H. P.; Sanders, J. C. P.; Schrobilgen, G. J. *J. Am. Chem. Soc.* **1991**, *113*, 3351−3361.
(2) Peacock, R. D.; Selig, H.; Sheft, I. *Proc. Chem. Soc., London* **1964**, 285.
(3) Peacock, R. D.; Selig, H.; Sheft, I. *J. Inorg. Nucl. Chem.* **1966**, *28*, 2561−2567.
(4) Christe, K. O.; Wilson, W. W. *Inorg. Chem.* **1982**, *21* (12), 4113−4117.
(5) Ellern, A.; Mahjoub, A. R.; Seppelt, K. *Angew. Chem., Int. Ed. Engl.* **1996**, *35* (10), 1123−1125.
(6) Hagiwara, R.; Hollander, F.; Maines, C.; Bartlett, N. *Eur. J. Solid State Inorg. Chem.* **1991**, *28*, 855−866.
(7) Tramšek, M.; Žemva, B. *Acta Chim. Slov.* **2006**, *53*, 105−116.
(8) Matsumoto, K.; Hagiwara, R.; Ito, Y.; Tamada, O. *Solid State Sci.* **2002**, *4*, 1465−1469.
(9) Grimes, R. N. *Inorganic Syntheses*; John Wiley & Sons: New York, 1992.
(10) Mazej, Z.; Žemva, B. *J. Fluorine Chem.* **2005**, *126*, 1432−1434.
(11) Peters, D.; Miethchen, R. *J. Fluorine Chem.* **1996**, *79*, 161−165.
(12) Frlec, B.; Gantar, D.; Holloway, J. *J. Fluorine Chem.* **1982**, *19*, 485−500.
(13) *CrystalClear*; Rigaku Corp.: The Woodlands, TX, 1999.
(14) Altomare, A.; Cascarano, G.; Giacovazzo, C.; Guagliardi, A. *J. Appl. Crystallogr.* **1993**, *26*, 343−350.
(15) Sheldrick, G. M. *Acta Crystallogr.* **2008**, *A64*, 112−122.
(16) Pearson, R. G. *Inorg. Chem.* **1988**, *27* (4), 734−740.
(17) Röhr, C.; Kniep, R. *Z. Naturforsch., B: Chem. Sci.* **1994**, *49*, 650−654.
(18) Burns, J. H. *Acta Crystallogr.* **1962**, *15*, 1098−1101.
(19) Graudejus, O.; Wilkinson, A. P.; Chacon, L. C.; Bartlett, N. *Inorg. Chem.* **2000**, *39* (13), 2794−2800.
(20) Fitz, H.; Müller, B. G.; Graudejus, O.; Bartlett, N. *Z. Anorg. Allg. Chem.* **2002**, *628* (1), 133−137.
(21) Tavčar, G.; Benkič, P.; Žemva, B. *Inorg. Chem.* **2004**, *43* (4), 1452−1457.
(22) Bunič, T.; Tavčar, G.; Tramšek, M.; Žemva, B. *Inorg. Chem.* **2006**, *45* (3), 1038−1042.
(23) Tramšek, M.; Benkič, P.; Žemva, B. *Inorg. Chem.* **2004**, *43* (2), 699−703.
(24) Tavčar, G.; Goreshnik, E.; Mazej, Z. *J. Fluorine Chem.* **2006**, *127* (10), 1368−1373.
(25) Mazej, Z.; Goreshnik, E. *Inorg. Chem.* **2008**, *47* (10), 4209−4214.
(26) Benkič, P.; Tramšek, M.; Žemva, B. *Solid State Sci.* **2002**, *4* (11−12), 1425−1434.
(27) Agron, P.; Begun, G.; Levy, H. *Science* **1963**, *139*, 842−843.
(28) Sladky, F. O.; Bulliner, P. A.; Bartlett, N. *J. Chem. Soc. A* **1969**, 2179−2188.
(29) Naulin, C.; Bougon, R. *J. Chem. Phys.* **1976**, *64*, 4155−4158.
(30) Gillespie, R. J.; Landa, B. *Inorg. Chem.* **1973**, *12*, 1383−1388.
(31) Gillespie, R. J.; Landa, B.; Schrobilgen, G. J. *Inorg. Chem.* **1976**, *15*, 1256−1263.
(32) Lehmann, J. F.; Dixon, D. A.; Schrobilgen, G. J. *Inorg. Chem.* **2001**, *40*, 3002−3017.